Studying the Operational Consequences of Automated Engine-Off Taxiing using Multi-Agent Planning

Explorative Case Study at Amsterdam Airport Schiphol

Malte von der Burg & Alexei Sharpanskykh
Air Transport Operations, Faculty of Aerospace Engineering
Delft University of Technology, The Netherlands
M.F.vonderBurg@tudelft.nl, O.A.Sharpanskykh@tudelft.nl

***Abstract*—Airports worldwide face a dual challenge towards 2050: meeting the predicted annual demand of 10 billion passengers, while striving for net-zero emissions throughout their operations. For airport surface movement operations, engine-off taxiing methods have the potential to cut the associated aircraft emissions. One promising technique is to use specialized tugs to tow aircraft to or from locations close to the runways. However, the implementation of tug-enabled taxiing (TET) introduces operational complexities, necessitating advanced planning, guidance, and control. Building upon prior research, we extend our existing multi-agent system model for automated taxiing operations to explore the operational implications posed by TET of all outbound flights with respect to the historic as well as automated multi-engine taxiing operations studied previously. We analyze the impact on taxi times, runway capacity, delay patterns, emission hotspots, and potential for fuel savings by simulating the real-world flight schedules of two of the busiest days at Amsterdam Airport Schiphol to date. In light of the considered simulation conditions, we show that TET greatly reduces the emissions in the bay areas, and decreases fuel consumption by up to 69%, resulting in estimated yearly fuel cost savings of 13.8 M€ at Schiphol. TET operations thus offer not only environmental and economic benefits, but have the potential to lower health-related risks for ground personnel as well.**

***Keywords*—airport surface movement operations; automation; engine-off taxiing; tug-enabled taxiing; multi-agent system; multi-agent motion planning; air traffic control**

I. Introduction

Airports around the world are facing two contrary challenges on the path to 2050: they must cope with the predicted demand of more than 10 billion yearly passengers, and must reduce their environmental footprint to fulfil the industry-wide goal of reaching net-zero emissions by the same time [1]. Achieving these opposed goals is even more challenging for large airports as it is expected that they cannot facilitate this growth with infrastructural expansions [2].

This work has received funding from the SESAR Joint Undertaking under grant agreement No 892869 under European Union's Horizon 2020 research and innovation programme.

Emissions during taxiing can effectively be reduced when aircraft do not use their engines during taxiing. The TaxiBot concept from IAI [3] is one of the most promising of such engine-off taxiing techniques [4]. A tug replaces the pushback-truck, and after pushback, continues to tow departing aircraft to a decoupling location close to the runway where the aircraft is decoupled from the tug. Since the tugs provide sufficient towing power, the aircraft engines can remain off, until the pilots have to start the engines to be ready to taxi onto the runway after decoupling.

In a feasibility study, Schiphol explored the potential consequences and open challenges to implement such tug-enabled taxiing (TET) for outbound flights throughout their operations [5], [6]. The study was based on the current infrastructure and processes, and highlighted the necessity for an advanced guidance and control system to counteract challenges such as queues forming on active taxiways due to tug decoupling.

Different aspects of airport surface movement operations (ASM Ops) were previously studied, including multi-objective routing [7], [8], automation [9], [10], and review of optimization approaches [11]. In prior work [12], we examined the operational consequences of automated ASM Ops, controlled by a multi-agent system with integrated routing algorithm to plan conflict-free trajectories and execute them accordingly. As suggested by [13], we included various processes such as pushback and engine-start explicitly in our model. Simulating the operations of two consecutive days at Amsterdam Airport Schiphol in July 2019 (two of the busiest days to date) resulted in 15% reduction of taxi times. However, to assess whether this operational control system is also suitable for TET operations, multiple questions remain, some of which are:

- How do TET operations affect key performance indicators like the taxi times of inbound and outbound flights as well as runway capacity?
- Does the long tug decoupling time of around two minutes lead to congestion and delays, especially when in-flow

decoupling is performed on busy taxiways?
- Do TET operations offer the potential to reduce fine particle emissions in the bay areas that pose a health risk for ground personnel [14]?

In this paper, we explore the potential operational impact that engine-off taxiing of outbound flights through the use of tugs poses. To this end, we extend the multi-agent system model from our previous work to simulate tug-enabled taxiing operations for the same flight schedule used in that study. The adapted model is described in Section II, and Section III explains the experimental setup. In Section IV, based on key performance indicators, we then compare tug-enabled taxiing (TET) to both historic and simulated multi-engine taxiing (MET) operations. Relating back to the open questions described above, we summarize our findings in Section V.

II. Multi-Agent System Model

The architecture of the multi-agent system (MAS) comprises both centralized and distributed agents that are organized in a distributed-hierarchical structure. Since we consider automated operations in this paper, we assume that the agents have full control and decision-making over the taxiing operations. Moreover, it is assumed that communication is done digitally through a datalink like AeroMACS, and that the A-SMGCS surveillance service is fully functional. The MAS is depicted in Fig. 1 and summarized in the following. Further details on the MAS and its verification and validation are provided in [12].

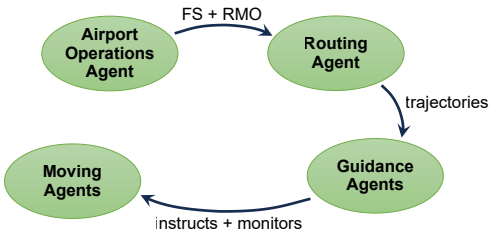

Figure 1. Overview of multi-agent system for automated multi-engine and tug-enabled taxiing operations, adapted from [12]

As shown in Fig. 2, we represent the taxiway layout of Amsterdam Airport Schiphol, which is used as case study in this paper, as graph G = (V, E) with vertices V and directional edges E. Vertices denote stands (green), intersections of taxiways (black) and service roads (blue), tug decoupling points (orange), tug all-clear points (grey, explained below), or stopbars in front of runway entries (red). The vertices are connected by two unidirectional edges to form a bidirectional segment of a taxiway (black) or service road (blue).

The centralized Airport Operations Agent determines the active runways based on the runway mode of operation (RMO). Since these must not be crossed by any vehicle, the respective

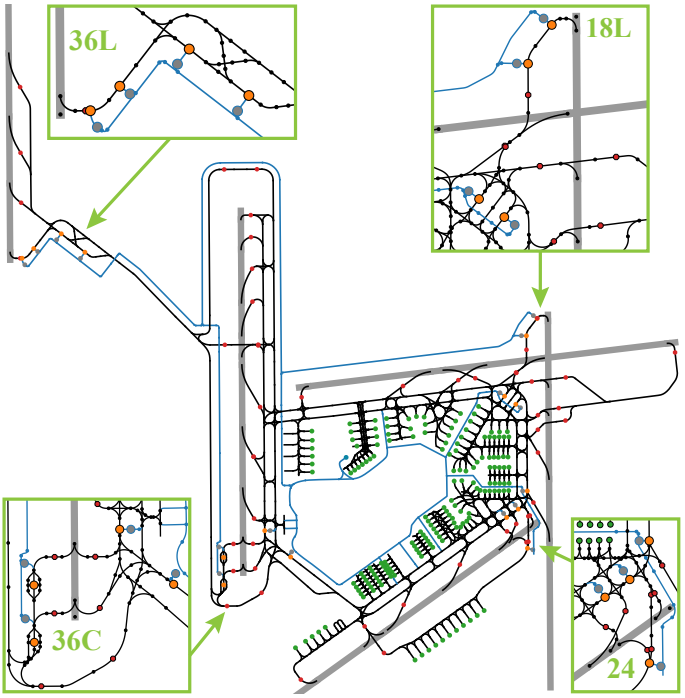

Figure 2. Graph of layout of Amsterdam Airport Schiphol with edges for runways (grey), taxiways (black), or service roads (blue), and vertices for gates (green), taxiway intersections (black), tug decoupling (orange) and all-clear points (grey), or stopbars (red)

taxiway segments are blocked by layout constraints. Furthermore, it sets the flight and tug schedules (FS), and revises them whenever an A-CDM milestone is updated.

The schedules and constraints are shared with the centralized Routing Agent that calculates conflict-free trajectories for all Moving Agents. A two-level motion planning search is deployed based on Priority-Based Search (PBS) [15] combined with an extended version of the Safe Interval Path Planning (SIPP) algorithm [16]. To ensure conflict-free paths, the algorithm accounts for the kinematics and shapes of agents, and resolves any conflicts within the planning window w_{plng}. The Routing Agent re-computes all plans once every replanning period h_{plng}, or after receiving updates from the Airport Operations Agent. Further details on the routing algorithm are provided in [12].

The conflict-free routes are shared with the Guidance Agents that are located at every intersection in the taxiway network and control those Moving Agents that are travelling towards their location. They send instructions to the Moving Agents under their control so that these are able to execute the route as planned. When the executed movements diverge from the planned trajectories, the Guidance Agents modify the instructed route to minimize the deviations. When the executed route differs much from the planned one, they request the Routing Agent to centrally replan the affected routes.

Moving Agents represent the (auto-)pilots and drivers of aircraft and tugs. They are assumed to be fully cooperative, i.e. execute instructions as closely as possible. To account for the various surface movement operations in path planning, the path of a Moving Agent is split into multiple activities based on go-to, follow, and wait activities, see [12] for further details.

For each Moving Agent, the Routing Agent uses a combination of these activities to define an activity sequence. Fig. 3 illustrates these sequences for arriving aircraft using multi-engine taxiing (MET), and departing aircraft using either MET or tug-enabled taxiing (TET). To finish the decoupling process as part of TET, a tug drives to a near all-clear point, and gives a signal that the pilot may continue taxiing. The tug then either drives back to its base or to the location of its next assignment.

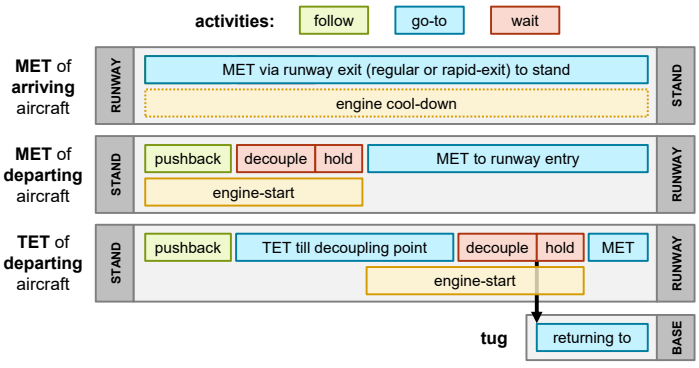

Figure 3. Activity sequence for arriving and departing aircraft. While engine-start (orange box) of departing aircraft is accounted for, engine cool-down (dotted orange box) is neglected.

The engine-warmup and engine-cooldown are special cases in the activity sequence of aircraft. During routing, the warmup-phase is accounted for as part of the engine-start manoeuvre, which is based on the aircraft-specific duration of its engine-start. In case that it takes longer to start the engine than the time till decoupling from the tug or pushback-truck, the trajectory includes additional holding either at the stand, the place of switching direction during pushback, or the decoupling location. Since the engine-cooldown of arriving aircraft does not have an influence on the routing, we neglect it and assume that it takes place after standstill at the stand.

In path planning, we represent the Moving Agents as circular shapes with a fixed radius, as listed in Table II in Section III. To limit the variety, we categorize all aircraft according to the six types listed in the ICAO aerodrome reference codes [17]. Tugs are assigned a fixed shape based on the TaxiBots as reference tug-system [18]. Moreover, we include a safety zone between agents, and account for minimal separation between takeoffs according to RECAT-EU [19].

III. Experimental Setup

In this section, we outline the experimental setup to compare the two taxiing modes of operation at Amsterdam Airport Schiphol for the historic flight schedules of the 17th and 18th July 2019. All experimental assumptions listed in [12] are valid for this study as well. Specifically for TET operations, we draw the following additional assumptions:

- all departing flights use TET, while arriving flights use MET
- tugs are fully electric, no fuel is required
- sufficient tugs are available, no task assignment is done
- tugs have to give way to all aircraft, i.e. path planning is done separately for tugs
- after decoupling, tugs can stay as long as necessary at all-clear points and are routed back to the tug base

Two primary runway mode of operations (RMOs) exist at Schiphol: **RMO North** (active on 17th July 2019), and **RMO South** (active on 18th July 2019). Throughout each day, different runway combinations are set, as described and illustrated in [12]. For the simulated operations, the same runways are active as during the historical operations. Runway 09/27 remained inactive during the two days. Flights to and from runway 04/22 are excluded, as these general aviation flights are primarily confined to Schiphol East. For both days, Table I provides details on the total number of flights, arrivals, departures, the main RMO, and the number of RMO phases.

TABLE I
Overview of Operational Data

date	17-07-2019	18-07-2019
flights	1489	1492
arrivals	745	744
departures	744	748
RMO	RMO North	RMO South
RMO phases	19	19

As mentioned earlier, each aircraft is assigned one of the six ICAO-types, each having a radius associated to its shape and a wake turbulence category (WTC). These parameters are listed in Table II along with the count per day. Tugs have a shape radius of $6\,\mathrm{m}$ and an unlimited number is available. Table III lists the kinematic properties of the Moving Agents and key algorithmic parameters. When aircraft are towed by a tug, the maximal velocity of tugs is applied. All agents have to keep a minimal safety distance from each other based on the average radius between each pair. Furthermore, when one agent is trailing another vehicle, it must maintain a safety distance of at least three times the shape radius of the preceding vehicle, determined through expert interviews.

To simulate tug-enabled taxiing (TET) operations, we made changes to the airport layout corresponding to the schedule data from 2019 to incorporate tug decoupling locations, all-clear

TABLE II
VEHICLE TYPES: NAME, SHAPE DIAMETER, WAKE TURBULENCE CATEGORY (WTC) FOR AIRCRAFT, AND COUNT IN OPERATIONAL DATA

	parameters		count per day	
	shape [m]	WTC	17-07-2019	18-07-2019
ICAO-A	12	CAT-F	0	0
ICAO-B	25	CAT-E	22	20
ICAO-C	40	CAT-D	1195	1198
ICAO-D	54	CAT-C	37	43
ICAO-E	72	CAT-B	213	206
ICAO-F	80	CAT-A	22	25
Tug	12	-	unlimited	

TABLE III
KINEMATIC PROPERTIES OF MOVING AGENTS AND ALGORITHM PARAMETERS THAT ARE USED IN THE ROUTING ALGORITHM

parameter	value	unit
maximal velocity aircraft $v_{max,AC}$	15	m/s
maximal velocity tugs $v_{max,GV}$	11.8	m/s
maximal turn velocity $v_{turn,max}$	5	m/s
minimal velocity v_{min}	1.5	m/s
acceleration acc	0.25	m/s^2
deceleration dec	-0.75	m/s^2
planning window w_{plng}	30	min
replanning period h_{plng}	15	min

points, and service roads for the return movements to their base, derived from interviews with operational experts. Furthermore, we included the second Quebec taxiway that was finished in 2022, which is important to facilitate tug decoupling close to the runway 36C. We thus refer to this layout as 2022+. The underlying graph has 1255 vertices and 3468 edges.

In the analysis, we compare different operational cases with each other: we use the historic operations and the automated multi-engine taxiing (MET) operations from [12] using the layout 2019 as reference. We show that the layout 2022+ has a negligible influence on the MET operations. This allows us to compare the TET operations on the layout 2022+ also to the historic operations. For TET operations, we use the operational limit of TaxiBots of $v_{max} = 11.8\,\mathrm{m/s}$. However, to aid our analysis, we also conducted a TET simulation using v_{max} from MET operations, and refer to this case as "TET (15m/s)".

To provide a rough estimate of the total fuel consumption, fuel costs, and CO_2 emissions, we use a fuel flow rate of $0.1\,\mathrm{kg/s}$ per engine based on the value for an A320 from [20]. We assume that all smaller aircraft (types ICAO-A, ICAO-B, and ICAO-C) use two engines, while the larger aircraft use four engines. During the engine-start duration of $3\,\mathrm{min}$ for smaller and $6\,\mathrm{min}$ for larger aircraft, we assume that half the fuel flow rate is necessary. To convert the accumulated fuel consumption into CO_2 emissions and fuel cost, we use $3.16\,\mathrm{kg\,CO_2/kg\,fuel}$ [21] and $0.8\,€/\mathrm{kg}$ [22], respectively.

IV. SIMULATION: RESULTS

To provide an overview of the traffic situation, Fig. 4 presents the hourly count of all flights for both multi-engine taxiing (MET) and tug-enabled taxiing (TET) operations over the two days of 17th and 18th July 2019. The two curves almost align, with MET operations displaying a slightly lower total count due to shorter taxi times, as discussed below. Additionally, the figure illustrates the count of arriving versus departing flights, showcasing the characteristic alternating trend between landings and takeoffs typical for a hub-and-spoke airport like Schiphol. In turn, this results in frequently changing RMO phases throughout the two days, represented by the colored shades in the figure.

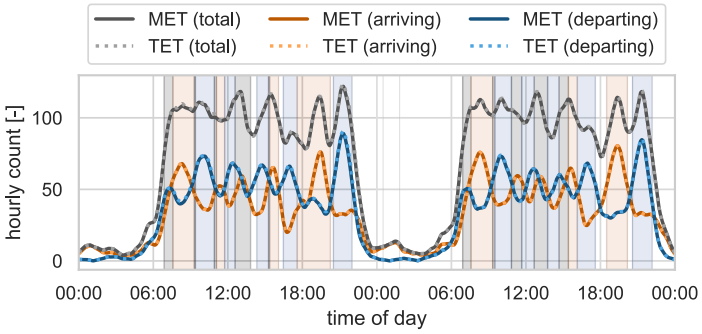

Figure 4. Hourly count of flights over the two days. Shades denote the RMO phase: off-peak (white), arrival-peak (orange), transition (grey), and departure-peak (blue)

Table IV lists multiple key performance indicators (KPIs) that we will use in the following sections to compare the historic, MET, and TET operations for both days. Besides the median taxi time $\tilde{t}_{taxi}$, we report the maximal throughput and occupancy rate per hour for any runway in use, and the total estimated consumption of jet fuel in tonnes. Note that the throughput and occupancy of arriving flights are identical for all three cases, since the simulated operations are based on the historic landing times.

TABLE IV
KPIS FOR HISTORIC, MULTI-ENGINE TAXIING (MET), AND TUG-ENABLED TAXIING (TET): MEDIAN TAXI TIME $\tilde{t}_{taxi}$, RUNWAY THROUGHPUT ($RWYthrpt.$) AND OCCUPANCY ($RWYocc.$) AS MAXIMAL HOURLY VALUE FOR ANY RUNWAY, AND ESTIMATED FUEL CONSUMPTION IN $[t]$

	date	17-07-2019			18-07-2019		
	operations	hist.	MET	TET	hist.	MET	TET
ARR	$\tilde{t}_{taxi}$	04:06	03:18	03:15	10:46	09:28	09:23
	RWY thrpt.		42			38	
	RWY occ.		68.7%			69.3%	
	fuel [t]	-	38.6	37.8	-	92.7	92.2
DEP	$\tilde{t}_{taxi}$	14:32	12:35	14:00	10:08	07:31	07:49
	RWY thrp.	45	44	46	43	42	42
	RWY occ.	74.7%	76.1%	78.8%	73.5%	76.6%	77.2%
	fuel [t]	-	115.0	35.8	-	62.3	35.8

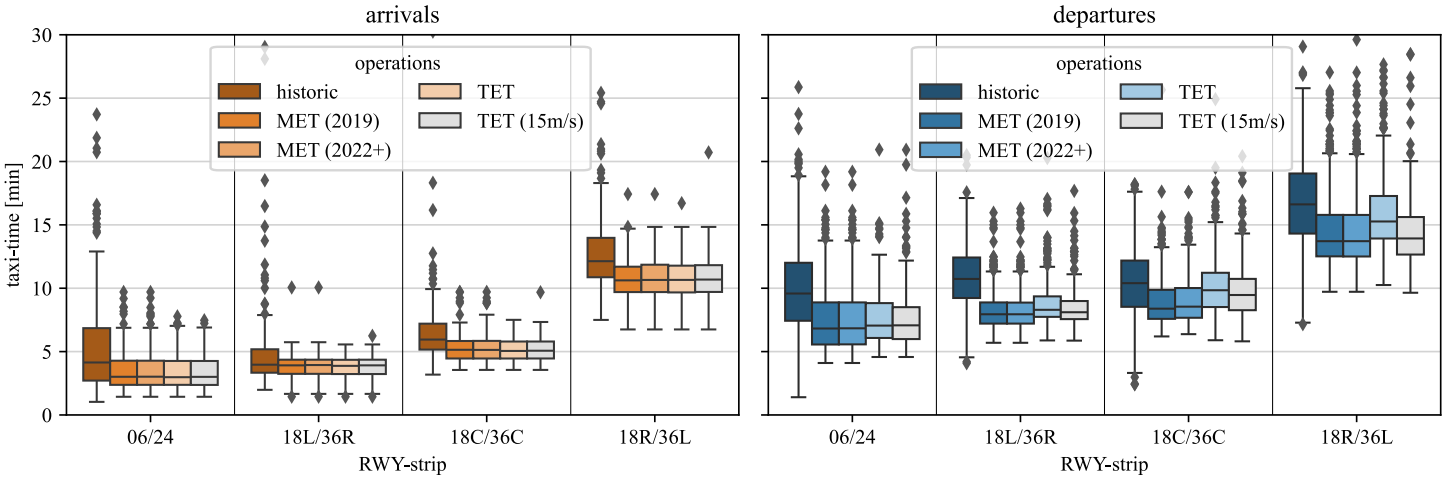

Figure 5. Box-and-whisker plot of historic and simulated taxi times for arrivals and departures per runway-strip

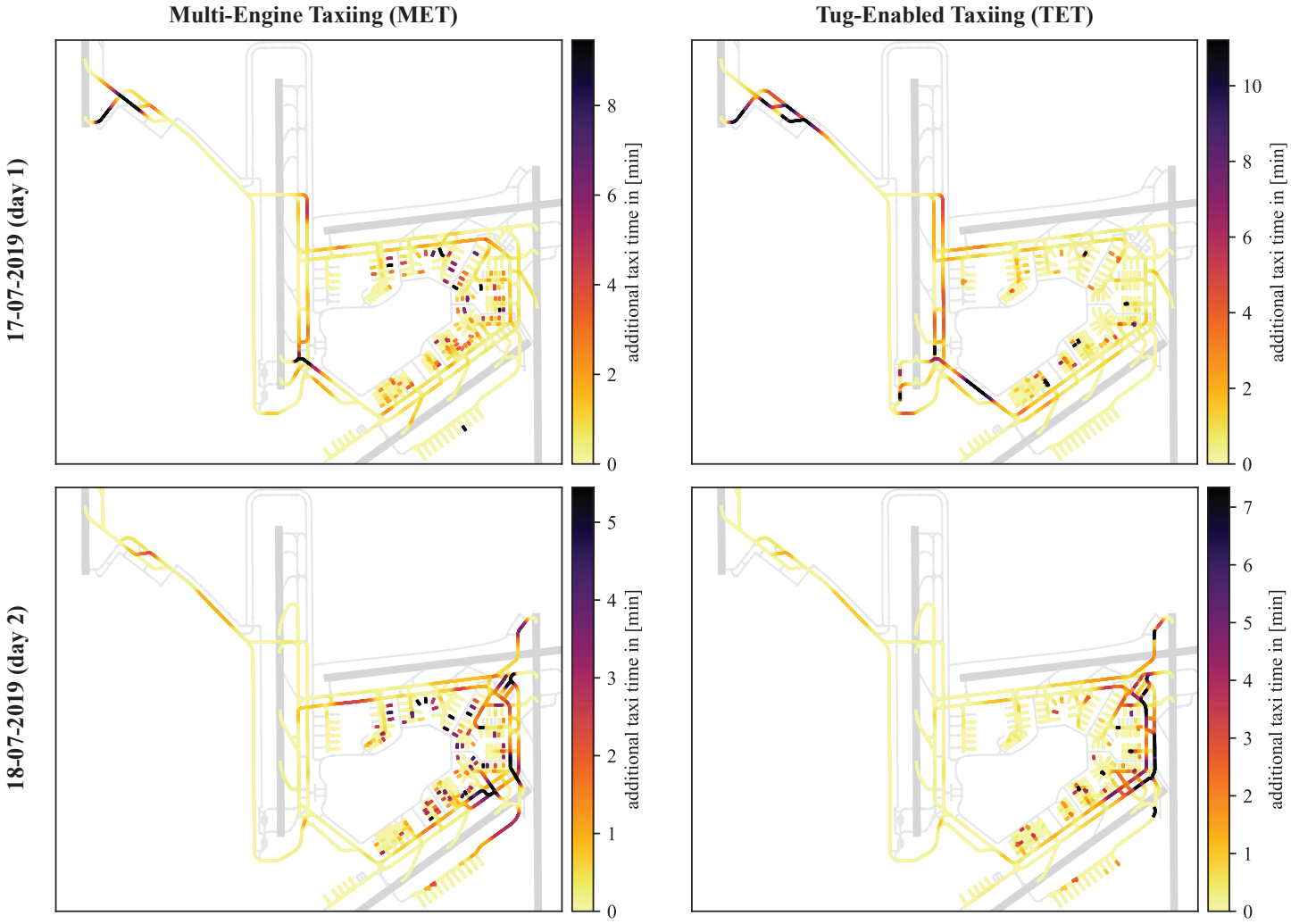

Figure 6. Delay hotspots depicted through additional taxi time per layout location for each day and each taxiing mode of operation

A. Comparison of Taxi Time Distributions per Runway

Fig. 5 shows the taxi times of the different operational cases both for arrivals (left) and departures (right) per runway strip as box-and-whisker plots, illustrating the median, first and third quartiles as box, as well as outliers as whiskers and points. For MET operations, the observations from [12] hold for both layout versions: the simulated operations have shorter and less varying taxi times for all runways, with taxi times of departing aircraft varying more due to the difference in engine-start durations between small and large aircraft. Since the taxi times are almost identically distributed, we conclude that the changes to the airport layout have a negligible effect on MET operations.

This allows us to compare TET operations on the adapted layout not only to MET but also to the historic values. Comparing MET to TET first, the taxi times of arriving aircraft are not affected by departing aircraft using TET. In contrast, the impact of TET varies for each departure runway strip: for runway 06/24, the taxi times are slightly higher but vary also slightly less. For 18L/36R and 18R/36L, the longer taxi times are mainly due to the smaller maximal velocity of tugs, confirmed by experiment "TET (15m/s)" that shows similar distributions to the MET case for both runways. The taxi times towards runway 18C/36C are longer and vary more, which is not only related to the smaller maximal velocity (as confirmed by experiment "TET (15m/s)"). This means that tug-enabled taxiing leads to higher inefficiencies specifically at this runway, most likely due to the placement and accessibility of the tug decoupling points.

In summary, while the TET operations do not have an impact on arriving flights compared to MET operations, they result in 11.3% and 4.0% higher median taxi times of departing aircraft on day 1 and day 2, respectively (cp. Table IV). However, in comparison to historic operations, the taxi times decrease by 3.7% on day 1 and 22.8% on day 2, and vary less between flights for all runways. Furthermore, as listed in Table IV, the maximal runway throughput and occupancy rate do not change significantly between historic, MET, and TET operations. The multi-agent system is thus able to keep the runway capacity not only for MET but also for TET operations.

B. Predictability of Taxi Time

In our previous work on automated airport surface movement operations (equal to MET operations in this paper) [12], we argued that accurate A-CDM milestones help to keep the different airport processes synchronized. Consequently, we analysed the predictability of the remaining taxi time provided by the Routing Agent throughout the operations. The same trends as discussed and depicted in Fig. 9 in [12] hold for TET operations. In summary, $30\,\mathrm{min}$ before reaching the taxiing destination, the predicted taxi time matches the actual taxi time of most flights, with some outliers showing deviations within $\pm 5\,\mathrm{min}$. No deviations occur within the last $10\,\mathrm{min}$ of taxiing.

C. Delay Hotspots in the Taxiway Network

As depicted in Fig. 6 and already observed in our previous study [12], MET operations show delay hotspots mostly in the bay areas due to engine-start and holding, the runway entries due to the necessary wake turbulence separation, and in front of the runway crossing of 18C/36C on the way to 18R/36L. In contrast, delays in TET operations occur mostly on the taxiways leading to a tug decoupling location. Furthermore, the delays are more concentrated as the accumulated delay is higher. While some holding still occurs in the bay areas, it is visibly much less than in MET operations.

Although the pattern close to runway 06/24 on day 2 differs between MET and TET, it does not impact the operations as confirmed by the similar taxi times discussed above. In comparison to day 1, more holding occurs in the bay areas: the decoupling locations are close to the bay areas and the flows to the two departure runways are more intertwined. Thus, the Routing Agent lets aircraft hold in bay areas to deconflict the concurrent routes.

D. Emission Hotspots in the Taxiway Network

For each day and for both MET and TET, Fig. 7 shows the accumulated time per layout location that engines of departing aircraft are starting or running, which provides insights into the areas in which exhaust emissions including fine particles are mostly produced during taxiing operations. For MET operations, the highest emissions are observable in the bay areas and the taxiways leading to the runway entries. In contrast, TET operations shift the emissions close to the runways. This is especially the case on day 1, in which only in one bay area low emissions (below $10\,\mathrm{min}$ over 24h) occur, while high emissions are concentrated in front and after the tug decoupling locations. On day 2, due to the short taxi distance to the decoupling locations in combination with the engine-start durations of $3\,\mathrm{min}$ for small and $6\,\mathrm{min}$ for large aircraft, low emissions still occur in most bay areas. Nonetheless, high emissions only arise around the decoupling locations.

E. Comparison of Engine-on Time per Runway

Fig. 8 displays the distribution of engine-on times of departing aircraft for the different simulated cases as box-and-whisker plots per runway-strip. Note that the fixed engine-start times are excluded, since they merely add an offset dependent on the aircraft type ($3\,\mathrm{min}$ vs. $6\,\mathrm{min}$). Furthermore, the engine-on times of arriving aircraft are not shown as they are identical to the taxi times from Fig. 5. While the engine-on times for departing flights using MET depend mostly on the distance between bay area and runway entry and thus the taxi time, the engine-on times for TET operations are similar for all runways, mostly between 1–$2\,\mathrm{min}$. They are also independent of the tug speed (confirmed by the case "TET (15m/s)"), since the engines are only fully

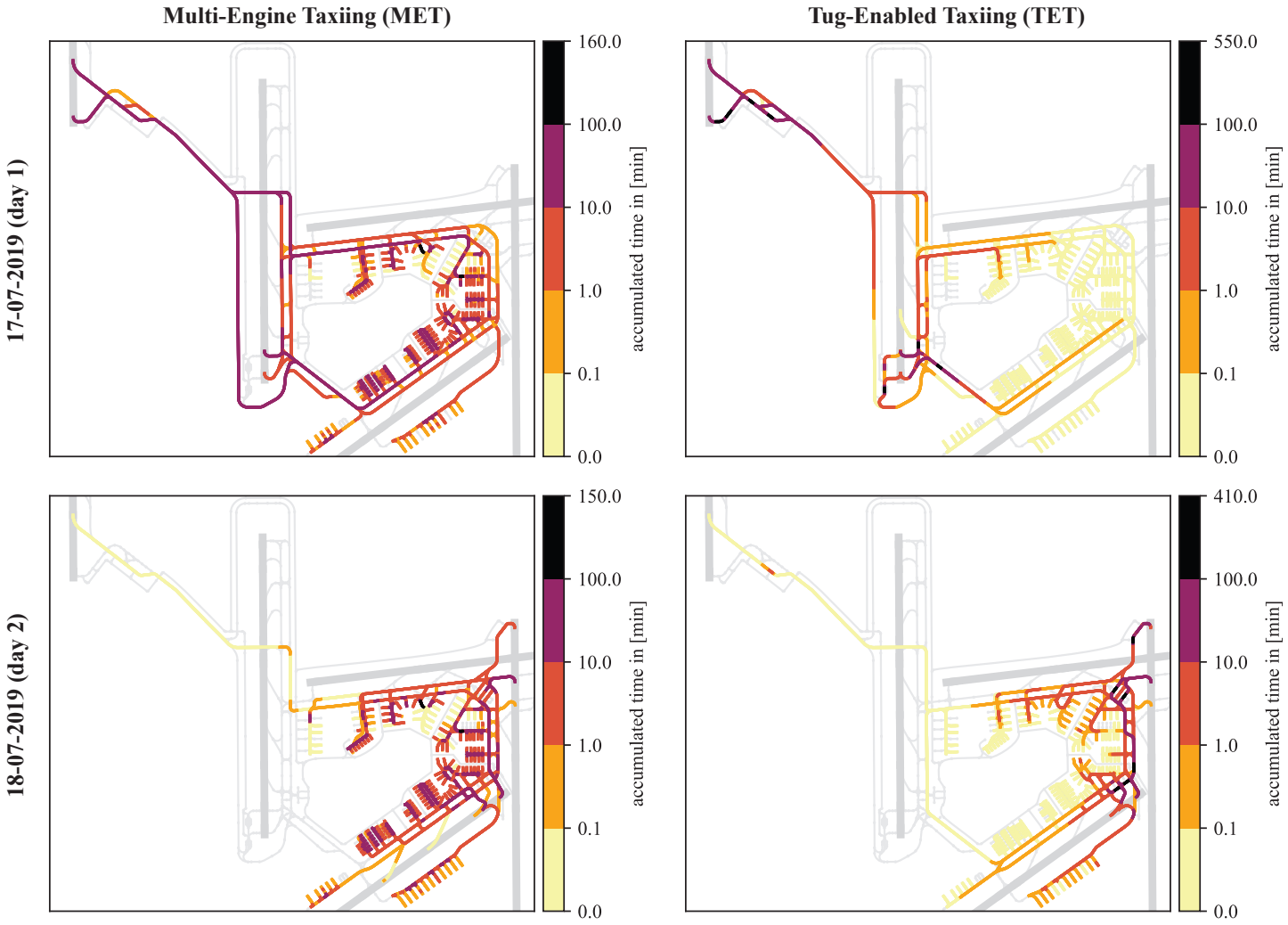

Figure 7. Emission hotspots depicted through accumulated engine on time per layout location for departing aircraft for each day and each taxiing mode of operation

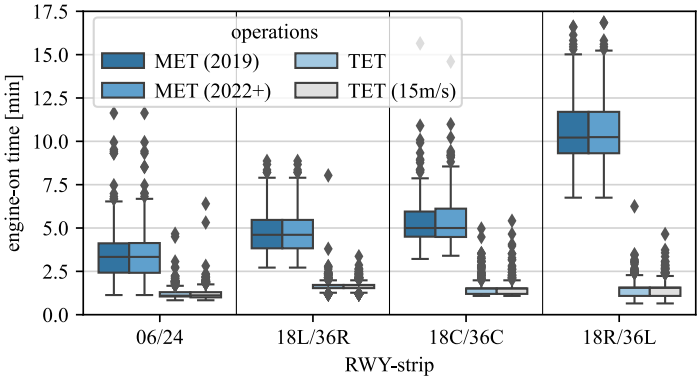

Figure 8. Box-and-whisker plot of engine-on times of departing flights per runway-strip

started after tug decoupling. Especially for runway 18R/36L, the engines thus only run a fraction of the times observed in the MET cases.

As rough estimate based on a fuel flow rate of $0.1\,\mathrm{kg/s}$ per engine, the total fuel consumption of departing flights decreases by 68.8% on day 1, and 42.5% on day 2 in comparison to MET operations. This reduces the CO_2 emissions by $250\,\mathrm{t}$ on day 1, and $84\,\mathrm{t}$ on day 2. For current jet fuel prices of $0.8\,€/\mathrm{kg}$, this also lowers the total fuel costs by $63\,\mathrm{T}€$ and $21\,\mathrm{T}€$ for the two days, respectively. Using the median fuel consumptions per runway and number of engines, we project this onto the pre-covid yearly movements of around 250k outbound flights at Schiphol: around $54.6\,\mathrm{kt}$ CO_2 emissions and $13.8\,\mathrm{M}€$ fuel costs could be saved per year, compared to MET operations. Since we used a rather low estimate of the fuel flow rate and did not model holding operations, the actual savings are likely higher.

F. Computational Efficiency of Routing Algorithm

Like our previous work, we used a Windows 10 laptop with 1.80 GHz Intel Core i7-10610U CPU and 16 GB RAM to run the Python-based simulations. For both MET and TET operations, the computational time increases exponentially with the number of agents. TET operations show slightly higher runtimes (mean: 42 s, 95th-percentile: 153 s, max: 435 s), likely because the algorithm must pick one of multiple tug decoupling locations as well as runway entry for departing flights, which increases the necessary computations.

G. Future Work

Based on this study, we plan to analyse different arrangements of the decoupling locations on the KPIs, especially those at runway 36C. Furthermore, we plan to study engine-off taxiing also for arriving aircraft to assess potential impact on the operations. Task assignment of tugs and directly routing them from a decoupling location to their next assignment are further directions.

Future research should also quantify different sources of uncertainty. Those with the highest impact should be included in path planning. Likewise, other ground vehicles that may especially impact the operations in the bay areas should be integrated into the model to study their impact.

V. Conclusion

In this paper, we explored the operational consequences that the use of tugs for engine-off taxiing of departing aircraft pose. All movements on the airport surface were coordinated and controlled by a hierarchical multi-agent system (MAS). Its architecture with conflict-free routing and Guidance Agents to provide instructions to the Moving Agents yielded safe operations.

We showed that the runway capacity was mostly unaffected by tug-enabled taxiing (TET). Although TET operations increase the taxi times towards runways far away from the bay areas, this is foremost due to the reduced taxiing speed of tugs. Compared to historic operations, the taxi times decreased by approx. 13%. TET operations did not affect the taxi times of inbound flights, yielding a reduction of around 16.7% compared to historic operations. The MAS thus efficiently coordinates the movements along the taxiway network and also around tug decoupling locations.

In comparison to multi-engine taxiing (MET), TET operations reduced the congestion around bay areas. Furthermore, the exhaust emissions including fine particles decreased significantly in bay areas. Besides, TET operations also decreased the fuel consumption of outbound flights by 68.8% for RMO North, and 42.5% for RMO South. At Schiphol, this yields estimated savings of 54.6 kt CO_2 emissions and 13.8 M€ fuel costs per year, based on current jet fuel prices. Therefore, TET operations offer the potential to significantly lower the environmental footprint of taxiing operations and health risks of ground personnel, while sustaining safety and efficiency levels.

References

[1] IATA. "Net-zero carbon emissions by 2050," Press Release No. 66. (2021), [Online]. Available: https://www.iata.org/en/pressroom/pressroom-archive/2021-releases/2021-10-04-03/ (visited on 04/04/2023).

[2] Eurocontrol, *European aviation in 2040 - challenges of growth*, Eurocontrol Statistics and Forecast Service, 2018.

[3] "TaxiBot Concept," TaxiBot International. (2023), [Online]. Available: https://taxibot-international.com/concept/ (visited on 02/07/2024).

[4] M. Lukic, P. Giangrande, A. Hebala, S. Nuzzo, and M. Galea, "Review, Challenges, and Future Developments of Electric Taxiing Systems," *IEEE Transactions on Transportation Electrification*, vol. 5, no. 4, 2019.

[5] D. Bresser and S. Prent. "The benefits of sustainable taxiing," Schiphol Innovation. (2020), [Online]. Available: https://www.schiphol.nl/en/innovation/page/the-benefits-of-sustainable-taxiing/ (visited on 02/05/2024).

[6] D. Bresser and S. Prent. "Is sustainable taxiing possible at a busy Schiphol?" Schiphol Innovation. (2021), [Online]. Available: https://www.schiphol.nl/en/innovation/blog/is-sustainable-taxiing-possible-at-a-busy-schiphol/ (visited on 02/05/2024).

[7] M. Weiszer, E. K. Burke, and J. Chen, "Multi-objective routing and scheduling for airport ground movement," *Transportation Research Part C: Emerging Technologies*, vol. 119, 2020.

[8] M. Zhang, Huang, Liu, and Li, "Multi-Objective Optimization of Aircraft Taxiing on the Airport Surface with Consideration to Taxiing Conflicts and the Airport Environment," *Sustainability*, vol. 11, 2019.

[9] P. C. Roling and H. G. Visser, "Optimal Airport Surface Traffic Planning Using Mixed-Integer Linear Programming," *International Journal of Aerospace Engineering*, vol. 2008, 2008.

[10] R. Morris and C. S. Pa, "Planning, Scheduling and Monitoring for Airport Surface Operations," *In AAAI-16 Workshop on Planning for Hybrid Systems*, 2016.

[11] J. A. D. Atkin, E. K. Burke, and S. Ravizza, "The Airport Ground Movement Problem: Past and Current Research and Future Directions," in *In 4th International Conference on Research in Air Transportation*, 2010.

[12] M. von der Burg and A. Sharpanskykh, "Multi-Agent Planning for Autonomous Airport Surface Movement Operations," in *SESAR Innovation Days 2023*, 2023.

[13] C. Stergianos, J. Atkin, P. Schittekat, T. Nordlander, C. Gerada, and H. Morvan, "The importance of considering pushback time and arrivals when routing departures on the ground at airports," in *Proceedings of ICAOR-16*, 2016.

[14] "Response by Schiphol to Labour Authority decision," Schiphol Newsroom. (2024), [Online]. Available: https://news.schiphol.com/response-by-schiphol-to-labour-authority-decision/ (visited on 02/06/2024).

[15] H. Ma, D. Harabor, P. J. Stuckey, J. Li, and S. Koenig, "Searching with consistent prioritization for multi-agent path finding," in *Proceedings of AAAI-19*, 2019.

[16] M. Phillips and M. Likhachev, "SIPP: Safe Interval Path Planning for dynamic environments," in *Proceedings of ICRA-11*, 2011.

[17] ICAO, "Aerodrome design and operations," in *Annex 14 to the Convention on International Civil Aviation*, ser. Aerodromes, 7th ed., 2016.

[18] "TaxiBot: The world's only certified and operational Taxiing alternative," TaxiBot. (2013), [Online]. Available: https://www.taxibot-international.com (visited on 05/10/2023).

[19] F. Rooseleer and V. Treve, *RECAT-EU: European wake turbulence categorisation and separation minima on approach and departure*, version 1.2, 2018, Released Issue.

[20] H. Khadilkar and H. Balakrishnan, "Estimation of aircraft taxi fuel burn using flight data recorder archives," *Transportation Research Part D: Transport and Environment*, vol. 17, no. 7, 2012.

[21] J. Overton, *The Growth in Greenhouse Gas Emissions from Commercial Aviation*, Environmental and Energy Study Institute, 2022.

[22] IATA. "Jet Fuel Price Monitor," Jet Fuel Price Monitor. (), [Online]. Available: https://www.iata.org/en/publications/economics/fuel-monitor/ (visited on 02/01/2024).